International Conference on Space Optics—ICSO 2010

Rhodes Island, Greece

4–8 October 2010

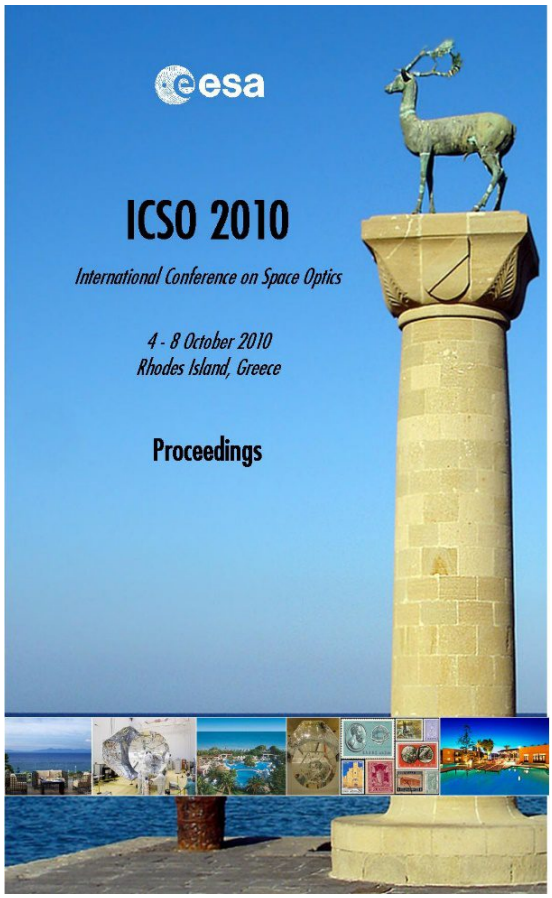

Edited by Errico Armandillo, Bruno Cugny, and Nikos Karafolas

Optical bench development for LISA

L. d'Arcio, J. Bogenstahl, M. Dehne, C. Diekmann, et al.

esa icso proceedings cnes

International Conference on Space Optics — ICSO 2010, edited by Errico Armandillo, Bruno Cugny, Nikos Karafolas, Proc. of SPIE Vol. 10565, 105652X · © 2010 ESA and CNES
CCC code: 0277-786X/17/$18 · doi: 10.1117/12.2309141

OPTICAL BENCH DEVELOPMENT FOR LISA

L. d'Arcio[5], J. Bogenstahl[3], M. Dehne[3], C. Diekmann[3], E. D. Fitzsimons[2], R. Fleddermann[3], E. Granova[3], G. Heinzel[3], H. Hogenhuis[4], C. J. Killow[2], M. Perreur-Lloyd[2], J. Pijnenburg[4], D. I. Robertson[2], A. Shoda[3], A. Sohmer[1], A. Taylor[2], M. Tröbs[3], G. Wanner[3], H. Ward[2], and D. Weise[1]

[1]*EADS Astrium GmbH - Satellites, 88039 Friedrichshafen, Germany*
[2]*University of Glasgow, Glasgow G12 8QQ, Scotland, UK*
[3]*Albert Einstein Institute, Callinstrasse 38, 30167 Hannover, Germany*
[4]*TNO Science & Industry, P.O. Box 155, 2600 AD Delft, The Netherlands*
[5]*ESA/ESTEC, Postbus 299, 2200 AG Noordwijk, The Netherlands*

Abstract

For observation of gravitational waves at frequencies between 30 µHz and 1 Hz, the LISA mission will be implemented in a triangular constellation of three identical spacecraft, which are mutually linked by laser interferometry in an active transponder scheme over a 5 million kilometer arm length. On the end point of each laser link, remote and local beam metrology with respect to inertial proof masses inside the spacecraft is realized by the LISA Optical Bench. It implements furthermore various ancillary functions such as point-ahead correction, acquisition sensing, transmit beam conditioning, and laser redundancy switching.

A comprehensive design of the Optical Bench has been developed, which includes all of the above mentioned functions and at the same time ensures manufacturability on the basis of hydroxide catalysis bonding, an ultrastable integration technology already perfected in the context of LISA's technology demonstrator mission LISA Pathfinder. Essential elements of this design have been validated by dedicated pre-investigations. These include the demonstration of polarizing heterodyne interferometry at the required Picometer and Nanoradian performance levels, the investigation of potential non-reciprocal noise sources in the so-called backlink fiber, as well as the development of a laser redundancy switch breadboard.

I. INTRODUCTION

The Laser Interferometer Space Antenna (LISA) is a cooperative space mission of ESA and NASA, aiming at the detection and observation of gravitational waves in a measurement band between 30 µHz and 1 Hz, in complement to ground-based gravitational wave detectors. LISA will be implemented in a constellation of three identical spacecraft at the corners of an equilateral triangle with a 5 million kilometer arm length, which is trailing Earth in a heliocentric orbit. Each spacecraft carries two free-falling reference targets, known as Proof Masses (PMs), defining the end points of the individual arms (Fig. 1). The passage of a gravitational wave causes minute fluctuations in the distance between the two proof masses of each arm, which are observed by heterodyne laser interferometry, that mutually links the three spacecraft in an active transponder scheme [1].

To allow for an independent technical optimization and decoupled verification of the individual functional elements of the metrology chain, the PM-to-PM interferometry on each interferometer arm is separated into two local and one long-arm measurement (Fig. 1): Relative motion of each PM with respect to its associated Optical Bench (OB) is detected by the **PM Optical Readout** (PM ORO) interferometer, while distance fluctuations between the two OBs of each interferometer arm are detected by the **Science Interferometer**. In this "strap-down architecture", each OB thus serves as the common fiducial reference for on-ground combination of all interferometric signals in a procedure known as Time Delay Interferometry (TDI). This effectively synthesizes a huge virtual interferometer from the metrology data collected over the entire constellation.

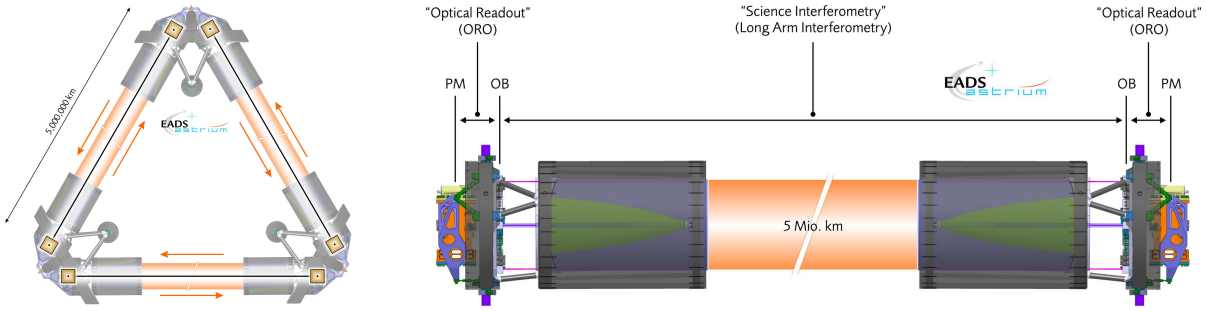

Fig. 1. *Left: Schematic of the LISA constellation. Each corner of the constellation triangle is delimited by the so-called Optical Assembly, which serves the two associated interferometer arms. Right: "Strap-Down Architecture". The proof-mass-to-proof-mass metrology on each arm is decomposed into essentially two local and one long arm measurement.*

As illustrated in Fig. 2, each OB interfaces optically on one side with the Gravitational Reference Sensor, and on its other side with an afocal telescope. Inside a contamination control enclosure, the Gravitational Reference Sensor houses the associated Proof Mass, a 46 mm^3 Gold-Platinum cube with a mass of 1.96 kg, which is electrostatically suspended in its rotational and lateral degrees of freedom. For optimization of the optical link budget on the long arm interferometry, the telescope provides an optical magnification of 80 to yield an external pupil of 400 mm diameter at the PM center of mass. It processes transmitted (TX) and received (RX) beam in opposite directions under a small point-ahead angle, required due to the non-negligible light travel time of approx. 16 s between the spacecraft [1].

Telescope Subsystem, Optical Bench, and Gravitational Reference Sensor are isostatically supported from a common interface ring to form the so-called Moving Optical Subassembly (MOSA), the main optical instrument of LISA. Each LISA spacecraft accommodates two identical MOSAs as part of the Optical Assembly, in which they can be individually rotated about a vertical pivot axis for precision pointing toward their respective remote counterpart.

II. OVERVIEW OF OPTICAL BENCH FUNCTIONS AND REQUIRED PERFORMANCE

The LISA OB supports a total of 4 interferometers, which are based on polarizing heterodyne interferometry in Mach-Zehnder-like configuration (Fig. 3). A total of three slightly separated continuous-wave, narrow linewidth laser frequencies near 1064 nm are processed on the OB to generate the associated heterodyne beat signals:

- **RX:** Laser light with a power of approx. 230 pW, received from the remote spacecraft in form of a plane wave, and clipped to a diameter of 5 mm by a dedicated aperture stop on the OB. Due to varying Doppler shifts caused by orbital dynamics, the observed RX frequency is continuously changing, so that beat frequencies in the range 2 - 19 MHz need to be accommodated on the OB.

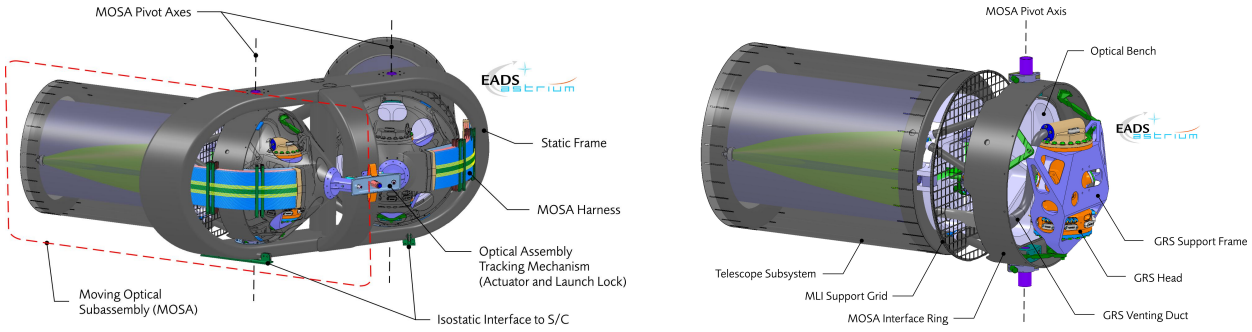

Fig. 2. *Left: Optical Assembly. Right: Each Optical Assembly consists of two identical Moving Optical Subassemblies (MOSAs), which can be fine-pointed to the location of their associated remote spacecraft.*

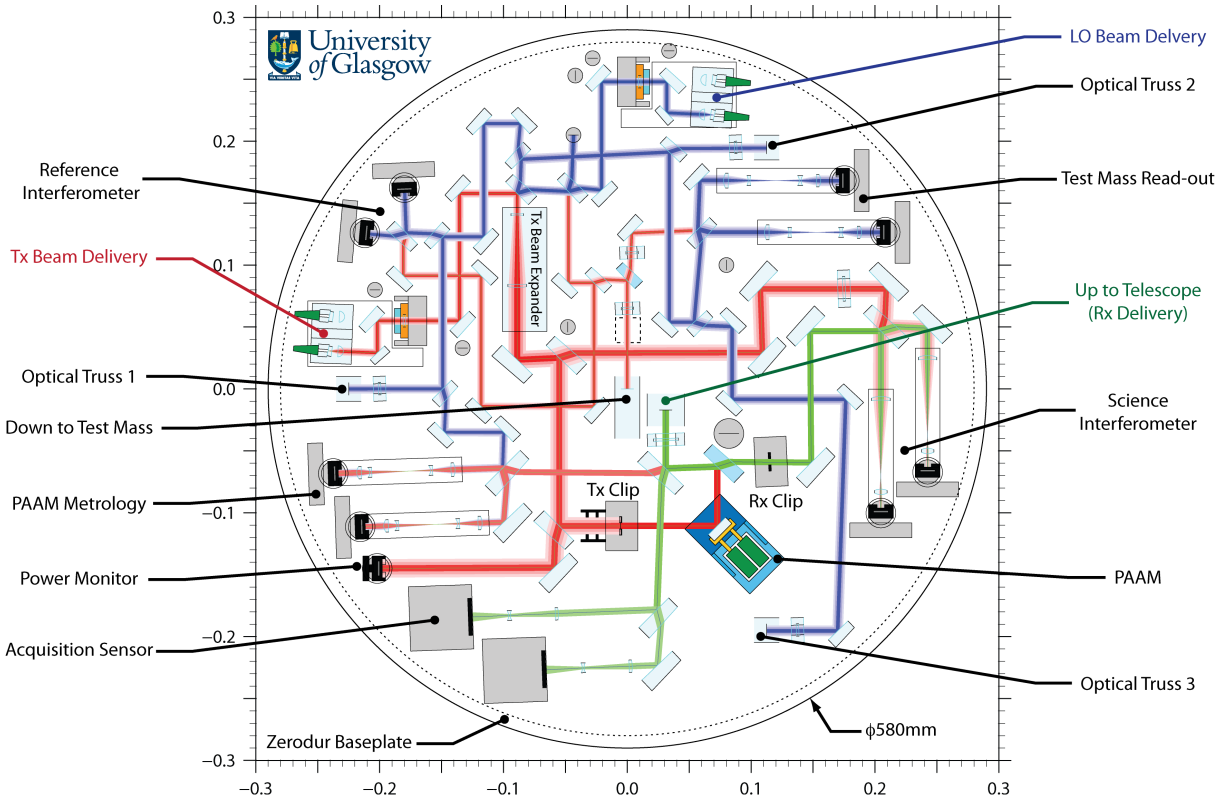

Fig. 3. *Optical Bench layout. Both standard and polarization beam splitters use wedged plate substrates made from Fused Silica, in order to minimize sources of spurious ghost beams. The optical elements will be integrated by a combination of hydroxide catalysis bonding [2] and adhesive bonding [3].*

- **TX:** Laser light with a power of approx. 1.2 W, delivered to the OB by singlemode, polarization maintaining fiber from the local Nd:YAG NPRO laser. While a small fraction is used for local interferometry, most of this light passes over the TX Aperture Stop and the Point-Ahead Angle Mechanism to be injected into the telescope for transmission to the remote spacecraft.
- **LO:** Laser light obtained from the TX laser on the second OB of the spacecraft via the so-called Backlink Fiber. This singlemode, polarization maintaining fiber allows to establish a phase reference between the two independent TX lasers on board each spacecraft, by carrying their light in opposite directions between the two OBs.

In the Science Interferometer, the phase of the weak RX beam is detected by mixing it with a fraction of the TX beam. This particular choice, known as non-frequency swap configuration, makes the Science Interferometer robust against stray light from the high power TX beam, if operated in balanced detection. All local interferometry employs particular combinations of TX and LO beams, to realize the previously mentioned PM ORO, the PAAM Metrology for detection of piston noise in the TX path, as well as a reference phase measurement. Apart from these interferometers, the LISA OB includes two further types of detectors: an Acquisition Sensor aiding initial acquisition of the RX beam over a larger field of view, and a Power Monitor for observation and active stabilization of the TX optical power.

For detection of beam pointing with Nanoradian precision, all interferometers on the LISA OB employ Differential Wavefront Sensing [4, 5]. This is realized by a spatially resolved phase measurement through the use of RF bandwidth Quadrant Photodetectors (QPDs). In order to decouple translation and tilt metrology as far as possible, dedicated imaging systems will be implemented in front of each QPD (Fig. 4). This approach, applied here to the best of our knowledge for the first time in an ultraprecise interferometric system, in particular minimizes pathlength measurement noise generated by pointing jitter of the measurement beams.

Nonetheless, such pointing jitter, originating from residual attitude dynamics of the spacecraft and the Proof Mass, remains one of the significant noise sources within the LISA system. The allowable pathlength measurement noise for LISA is generally expressed in form of a single-link budget from local to remote proof mass on

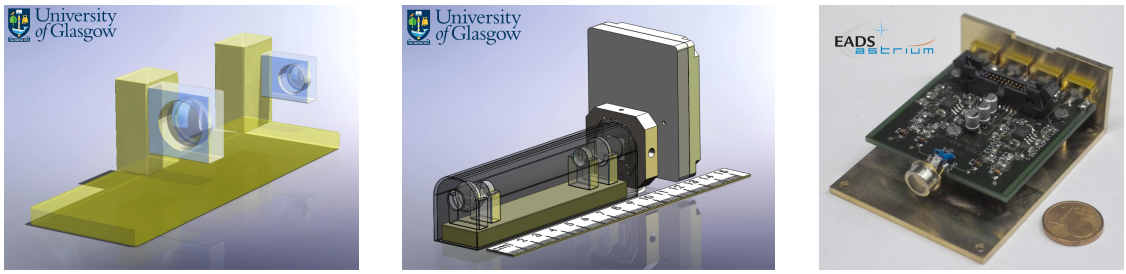

Fig. 4. *Left: Lens mounting concept providing all required degrees of freedom in combination with hydroxide catalysis bonding. Middle: Interferometric Detector Assembly, comprising imaging system and Quadrant Photodetector. Right: Prototype QPD employing an InGaAs photodiode with an active diameter of 1 mm.*

each arm, in direct correspondence to the strap-down concept introduced above. From the total single-link noise budget of

$$12\,\frac{\mathrm{pm}}{\sqrt{\mathrm{Hz}}} \times \sqrt{1+\left(\frac{2.8\,\mathrm{mHz}}{f}\right)^4}, \tag{1}$$

where f is the frequency of the spectral noise component, the following allocations may be mapped to contributions from the Optical Bench Subsystem:

Error Source	Allocation @ 5 mHz
Long Arm Interferometry (including full TX and RX paths on the OB)	$8.72\,\mathrm{pm}/\sqrt{\mathrm{Hz}}$
Proof Mass Optical Readout (per Proof Mass)	$1.42\mathrm{pm}/\sqrt{\mathrm{Hz}}$
Coupling of Spacecraft Attitude Dynamics to RX piston on Science Interferometer	$1.20\,\mathrm{pm}/\sqrt{\mathrm{Hz}}$
Coupling of Spacecraft Attitude Dynamics to TX piston in far field	$1.20\,\mathrm{pm}/\sqrt{\mathrm{Hz}}$
Coupling of Proof Mass Attitude Dynamics to PM ORO piston	$1.06\,\mathrm{pm}/\sqrt{\mathrm{Hz}}$
Total Budget for a single OB	$9.06\,\mathrm{pm}/\sqrt{\mathrm{Hz}}$

The allocations above for Long Arm Interferometry and Proof Mass Optical Readout refer to the pathlength measurement noise for *static* measurement beams, i. e. they do not include contributions from pointing jitter, which are covered by the remaining entries. The most dominant noise source is shot noise in the long arm interferometry, with a contribution of approx. $8.13\,\mathrm{pm}/\sqrt{\mathrm{Hz}}$.

III. BREADBOARD STUDIES

The local Nd:YAG laser providing the TX beam is backed by an identical second unit, which is operated in cold redundancy. Each of these two lasers has a separate fiber connection to a Fiber Switching Unit (FSU) on the associated OB, which implements free beam redundancy switching between the two inputs. As illustrated in Fig. 5, this is realized by combining the output of the associated fiber collimators at a polarizing plate beam splitter, and correction of the polarization by rotation of a half wave plate, with subsequent polarization cleanup in a second non-absorptive polarizer.

Essential novel features of the FSU have been investigated and validated by development and realization of dedicated breadboards. Beam collimation to an extremely low rms wavefront error of about $\lambda/37$ has been demonstrated by prototyping a so-called Fiber Mounted Assembly (FMA), and combining it with an aspherical collimating lens made from Fused Silica, which was precision aligned by use of a hexapod (Fig. 5). This result thus provides a proof of feasibility for achieving the required beam quality of $\lambda/30$ in the TX beam, which ensures compliance to the noise allocation for coupling of spacecraft attitude dynamics to TX piston in the far field, as quoted in the above noise budget.

Wave plate rotation within the FSU is performed on the basis of piezo-activated slip-stick motion in a specifically developed FSU Actuator (Fig. 6), which has been fully qualified both with respect to sub-µradian pointing reproducibility and environmental load cases. A second type of mechanism installed on the OB is the Point-Ahead Angle Mechanism (PAAM), of which a fully validated prototype is illustrated in Fig. 7. While maintaining

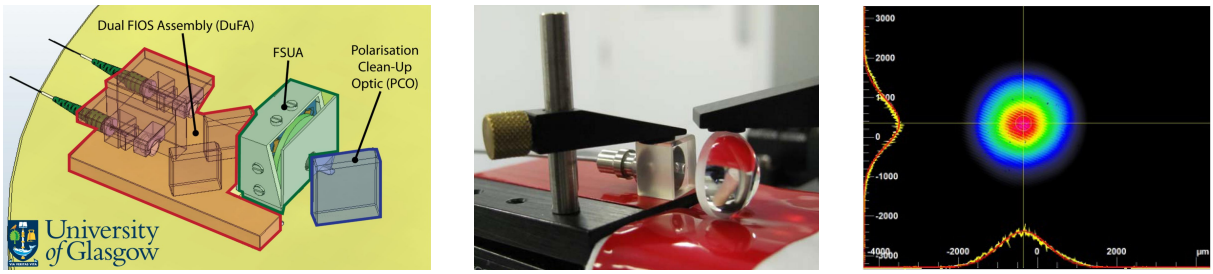

Fig. 5. *Left: Fiber Switching Unit, comprising a Dual FIOS Assembly for combination of the two redundant fiber inputs, the FSU Actuator (FSUA), and subsequent Polarization Cleanup Optics. Middle: Breadboard of a Fiber Injector Optical Subassembly (FIOS), consisting of the Fiber Mounted Assembly (FMA) and a collimating lens. Right: Beam quality obtained from this FIOS.*

picometer pathlength stability within the measurement band, it allows a single-axis adjustment of the out-of-plane point-ahead angle, which exhibits a quasi-periodic variation with a one-year period due to orbital dynamics [1]. An active correction is required, since the variation with an amplitude of approx. ±6 µrad is significantly larger than the far-field beam width of 3.1 µrad FWHM.

IV. EXPERIMENTAL VALIDATION OF METROLOGY PRINCIPLES

The metrology principles fundamental to the architecture of the Optical Bench as outlined above have been validated by a number of targeted experimental studies, of which a selection is addressed in the following.

Since the performance of polarizing heterodyne interferometry can principally be limited by periodic non-linearities and other effects potentially not present in a polarization-insensitive setup, a particular focus has been a quantitative comparison between these two beam routing alternatives at representative performance levels. A specific interferometric setup was devised for this purpose, comprising a polarizing as well as a non-polarizing Mach-Zehnder interferometer observing effectively identical measurement paths, as illustrated in Fig. 8. The interferometer core was integrated on a Clearceram-HS® baseplate using hydroxide-catalysis bonding. Since the measurement performance curves depicted in Fig. 8 show no significant difference between the polarizing and the non-polarizing interferometer, and are all very close to a noise level of $1\,\mathrm{pm}/\sqrt{\mathrm{Hz}}$, the principal applicability of polarizing heterodyne interferometry for LISA is thus demonstrated.

The Backlink Fiber transporting the TX light from the two OBs on board each spacecraft in opposite directions has to be fully reciprocal, i. e. the fiducial error resulting from a difference in the two counter-propagating optical paths is required to remain below $1\,\mathrm{pm}/\sqrt{\mathrm{Hz}}$ within the LISA measurement band. This crucial property of the Backlink Fiber has been validated as schematically illustrated in Fig. 9. The setup employs again a quasi-monolithic, fully bonded interferometer on a Zerodur baseplate, which mimics the actual situation on the LISA OB as far as possible. Essential to demonstrating a reciprocity to picometer level in this experiment has been the application of so-called normalized straylight correction using balanced detection, as well as a subtraction of pathlength noise correlated with excessive environmental temperature fluctuations.

Taking into account results from further on-going experiments, including in particular the principal validation

Fig. 6. *FSUA Breadboard on a Zerodur test carrier.*

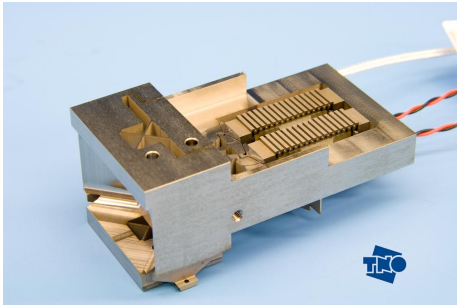

Fig. 7. *Point-Ahead Angle Mechanism.*

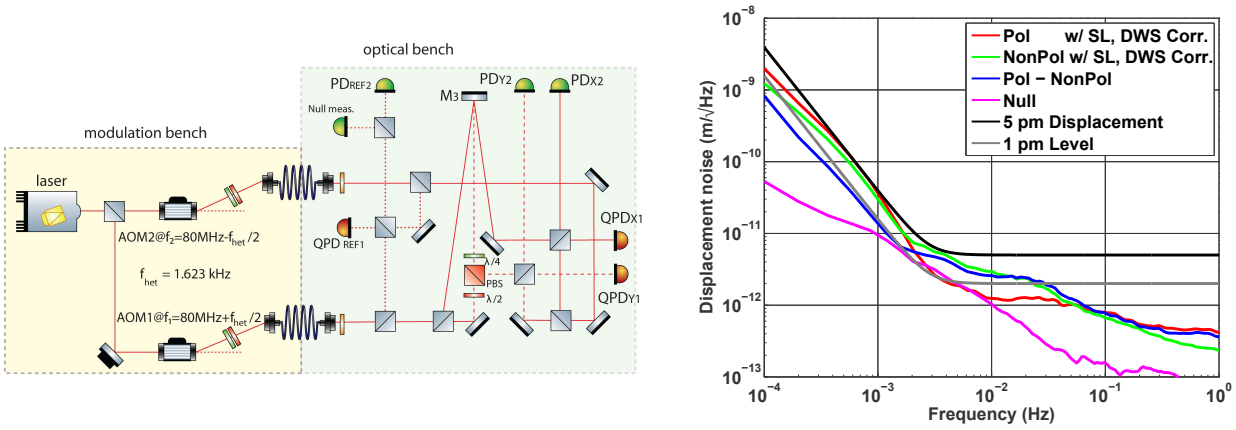

Fig. 8. *Left: Experimental setup for performance verification of polarizing heterodyne interferometry. Right: Measurement performance obtained in a noise measurement, with static measurement mirror M3.*

of the interferometric imaging approach, it may be concluded that the basic metrology principles to be applied on the LISA OB are principally validated, so that in a next step an Elegant Breadboard of the LISA OB will be fully designed and realized on the basis of these.

REFERENCES

[1] D. Weise, P. Marenaci, P. Weimer, M. Berger, H. R. Schulte, P. Gath, and U. Johann. Opto-mechanical architecture of the LISA instrument. In *ICSO Conference Proceedings*, 2008.

[2] E. J. Elliffe, J. Bogenstahl, A. Deshpande, J. Hough, C. Killow, S. Reid, D. Robertson, S. Rowan, H. Ward, and G. Cagnoli. Hydroxide-catalysis bonding for stable optical systems for space. *Class. Quantum Grav.*, 22:S257, 2005.

[3] S. Ressel, M. Gohlke, D. Rauen, T. Schuldt, W. Kronast, U. Mescheder, U. Johann, D. Weise, and C. Braxmaier. Ultrastable assembly and integration technology for ground- and space-based optical systems. *Applied Optics*, 49(22):4296, 2010.

[4] E. Morrison, B. J. Meers, D. I. Robertson, and H. Ward. Automatic alignment of optical interferometers. *Applied Optics*, 33(22):5041, 1994.

[5] E. Morrison, B. J. Meers, D. I. Robertson, and H. Ward. Experimental demonstration of an automatic alignment system for optical interferometers. *Applied Optics*, 33(22):5037, 1994.

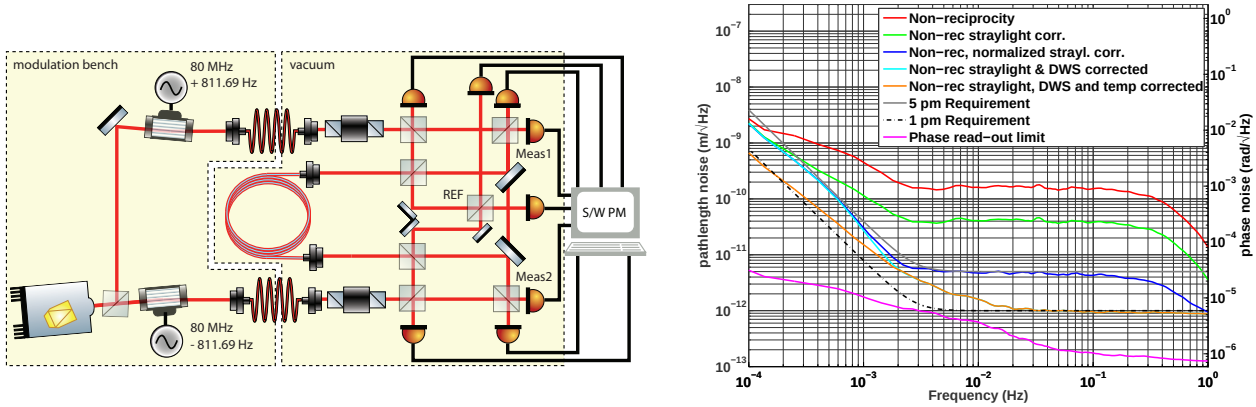

Fig. 9. *Left: Experimental setup for investigation of non-reciprocities iin the backlink fiber. Right: Measured non-reciprocity.*